Hybrid Expert–Machine Learning Weighting for GIS-Based Photovoltaic Suitability Mapping: A Spatial Robustness Assessment under Uncertainty

Kamran Ali[1], Eliseo Clementini[2], Roberto Patrizi[3], Carlo Villante[2]

[1] Dept. of Industrial and Information Engineering and Economics, University of L'Aquila, Italy - kamran.ali@graduate.univaq.it
[2] Dept. of Industrial and Information Engineering and Economics, University of L'Aquila, Italy - (eliseo.clementini, carlo.villante)@univaq.it
[3] Rainbow Lab srl, Viale Giulio Cesare 94, 00192 Roma, Italy - roberto.patrizi@rainbow-lab.it

Keywords: Photovoltaic Suitability, GIS–MCDM, Hybrid Weighting, AHP–XGBoost, Monte Carlo Robustness, Tornado Sensitivity Analysis

Abstract

Geographic Information Systems and Multi-Criteria Decision-Making (GIS–MCDM) workflows are widely used for photovoltaic (PV) site suitability mapping, but their outputs depend strongly on criterion weights, and many studies report deterministic suitability maps without testing whether priority zones remain stable under weight uncertainty. This study combines expert-derived weights from the Analytic Hierarchy Process (AHP, consistency ratio = 0.0142) with SHAP-based feature importance from an XGBoost model trained on 72 existing PV plants (ROC–AUC = 0.9391) to construct a hybrid weighting scheme ($\alpha = 0.7$), applied through SAW, TOPSIS, and VIKOR to map PV suitability in the Province of L'Aquila, Italy. Spatial robustness is assessed using 1,000 Monte Carlo weight perturbations and Tornado-style sensitivity analysis. Results show a clear stability gradient across the aggregation methods, with mean coefficient of variation values of 0.046, 0.121, and 0.193 for SAW, TOPSIS, and VIKOR, respectively. The top-suitability probability maps identify spatially concentrated high-suitability cores that persist across the three methods, while the Tornado analysis shows that GHI, urban distance, and slope exert the strongest control on spatial stability: the same criteria for which expert-derived and data-driven weights disagree most. By distinguishing robust priority zones from sensitivity-prone areas and identifying the criteria that govern spatial stability, the framework provides a defensible, uncertainty-aware workflow for PV siting and spatial energy planning.

1. Introduction

The transition towards low-carbon energy systems is a defining priority of international climate policy, reinforced at COP28 by the commitment to accelerate renewable deployment towards mid-century net-zero targets (UNFCCC, 2023). Solar photovoltaic (PV) generation has expanded rapidly worldwide on sustained cost reductions and technological maturity, and now plays a central role in decarbonising national energy portfolios (IRENA, 2024), while also supporting local economic activity and energy security (Hanna et al., 2024). Realising this potential at the utility scale, however, depends critically on site location because energy yield, grid-integration cost, and environmental compatibility are strongly location-dependent. Poorly sited installations can therefore create land-use conflicts and ecological impacts (Aydin et al., 2013; Heo et al., 2021).

PV site selection is therefore an inherently spatial problem. Suitability depends simultaneously on solar resource, terrain, land-cover compatibility, accessibility to road and grid infrastructure, proximity to urban and industrial areas, environmental buffers around waterways, and seasonal constraints such as snow frequency. These criteria are heterogeneous, expressed in different units, and often in conflict, so suitability cannot be reduced to a single factor (Heo et al., 2021; Villacreses et al., 2022). Geographic Information Systems coupled with Multi-Criteria Decision-Making (GIS–MCDM) provide a widely used spatial decision-support framework for renewable energy siting, integrating environmental, technical, infrastructural, and regulatory criteria within a structured, spatially explicit evaluation (Malczewski, 2006; Sahoo et al., 2025).

Within these workflows, criterion weighting is a key step because it controls the relative contribution of each criterion to the final suitability map. Expert-driven weighting, particularly the Analytic Hierarchy Process (AHP) and its fuzzy extension (FAHP), is widely applied for solar and PV siting (Merrouni et al., 2018; Hosouli and Hassani, 2024), offering interpretability and a structured decision logic grounded in domain expertise. However, AHP weights are derived from subjective pairwise comparisons and depend heavily on the analyst's judgment; even FAHP, which adds fuzzy logic to represent imprecision, still reflects human assessment rather than empirical spatial evidence (Hosouli and Hassani, 2024; Saaty, 1990).

To reduce this dependence on subjective judgment, machine learning has increasingly been used to extract data-driven evidence from the observed distribution of existing PV installations. Feature-importance techniques quantify the empirical contribution of siting factors directly from deployment patterns, providing an objective complement to expert weighting (Sun et al., 2023; Sari and Yalcin, 2024). This objectivity comes at a cost: purely data-driven models can overfit and offer limited interpretability, constraining their acceptance in planning contexts where decisions must be explainable to stakeholders (Hastie et al., 2009; Rudin, 2019). A hybrid strategy that combines AHP-based expert judgment with machine-learning-derived feature importance offers a balanced alternative, preserving the structured reasoning and interpretability of expert methods while incorporating empirical evidence from existing PV installations, reducing subjectivity without sacrificing transparency (Sun et al., 2023; Sari and Yalcin, 2024).

https://doi.org/10.5194/isprs-archives-L-4-W3-2026-1-2026

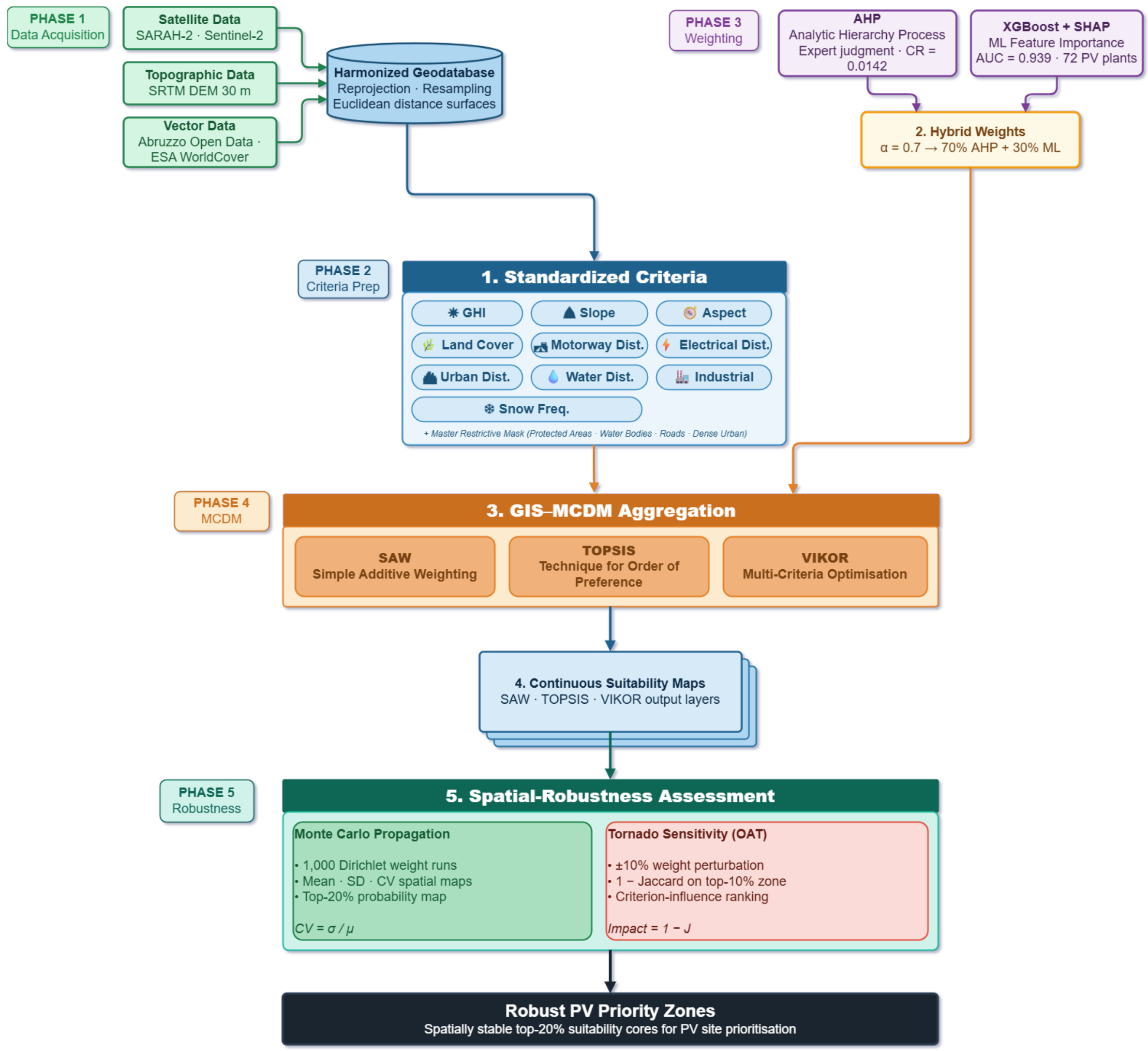

Figure 1. Overall methodological framework for hybrid GIS–MCDM PV site suitability mapping with spatial-robustness assessment.

Improving the weighting process does not by itself ensure reliable maps: the highest-ranked zones are sensitive to the exact weight values, so even small weight changes can alter the suitability pattern (Feizizadeh and Blaschke, 2014; Ligmann-Zielinska and Jankowski, 2014). Because expert-derived and hybrid weights are point estimates based on judgment or finite samples, a single deterministic map may hide uncertainty and overstate decision stability (Ligmann-Zielinska and Jankowski, 2014). Testing this uncertainty is therefore essential before treating high-suitability zones as reliable planning priorities (Feizizadeh and Blaschke, 2014; Ligmann-Zielinska and Jankowski, 2014; Al Garni and Awasthi, 2020). Monte Carlo simulation propagates weight uncertainty into ensembles of suitability outputs, while one-at-a-time methods rank the criteria that most drive output variation (Al Garni and Awasthi, 2020). Yet many GIS–MCDM PV studies still report a single map without testing whether the identified zones remain spatially stable when criterion weights are perturbed within plausible bounds, even though a high-suitability area is meaningful only if it stays suitable under that uncertainty.

To address this gap, the present study adds an explicit robustness assessment to the hybrid-weighted GIS–MCDM workflow. Monte Carlo simulation is used to test whether high-suitability zones remain stable when criterion weights are perturbed, producing mean, coefficient of variation, and top-suitability probability maps (Feizizadeh and Blaschke, 2014; Al Garni and Awasthi, 2020). A complementary Tornado-style one-at-a-time analysis then identifies which criteria cause the largest spatial changes in the high-suitability zones, providing a criterion-influence ranking rather than only a descriptive sensitivity plot (Al Garni and Awasthi, 2020).

The research has four objectives: to implement a hybrid AHP–machine-learning weighting framework for PV suitability mapping; to generate and compare suitability maps using the SAW, TOPSIS, and VIKOR algorithms; to assess the spatial robustness of these outputs under criterion-weight uncertainty using Monte Carlo simulation; and to identify, through Tornado-style sensitivity analysis, the criteria that most control the stability of high-suitability zones.

This study forms part of a broader research programme on PV development and monitoring in the Province of L'Aquila. It extends the GIS–MCDM siting framework of Clementini et al. (2024) with hybrid AHP–machine-learning weighting and an explicit robustness assessment, complementing related work on the monitoring and operational stages of the PV lifecycle (Ali et al., 2025a,b, 2026). The workflow is summarised in Fig. 1.

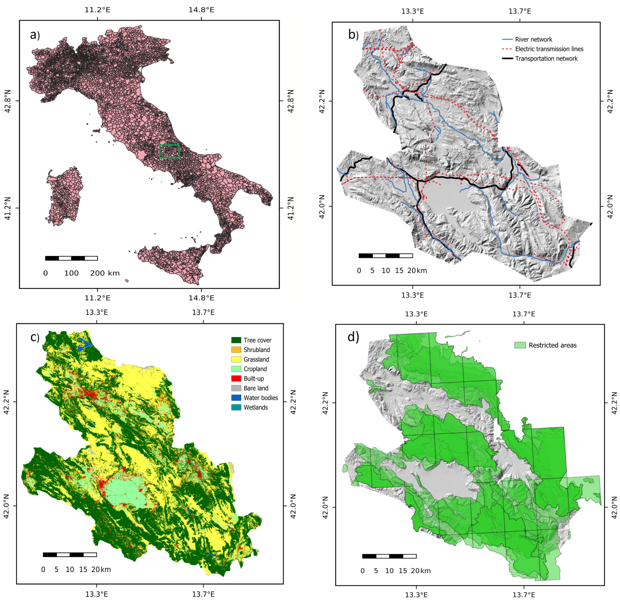

Figure 2. Study area — Province of L'Aquila, Italy: (a) location within Italy; (b) terrain hillshade with infrastructure networks; (c) land use/land-cover (LULC); (d) restricted areas.

2. Study Area and Data

2.1 Study Area

This study focuses on the Province of L'Aquila, in the Abruzzo region of central Italy, centred approximately at 42.35° N, 13.40° E (Fig. 2). The analysis boundary covers about 5,048 km^2 across the central Apennine mountain system. Elevations range from valley floors below 300 m to peaks exceeding 2,000 m, producing marked spatial differences in slope, aspect, accessibility, and solar exposure. Land-cover is equally diverse: built-up areas, agricultural land, pastures, forests, shrublands, and environmentally sensitive zones occur within short distances of one another, while roads, electric transmission lines, waterways, and industrial zones are spatially uneven. This combination of mountainous terrain, heterogeneous land-cover, seasonal snow, and uneven infrastructure makes the province a suitable test area for assessing the spatial robustness of hybrid-weighted GIS–MCDM PV suitability outputs under criterion-weight uncertainty.

2.2 Data and Criteria Selection

The evaluation criteria were selected based on established PV site-selection literature (Aydin et al., 2013; Sahoo et al., 2025; Villacreses et al., 2022), the availability of authoritative spatial datasets, and the physical characteristics of the Province of L'Aquila. They represent the principal dimensions governing utility-scale PV feasibility: solar resource potential, topographic feasibility, land-use compatibility, environmental constraints, and infrastructure accessibility. Ten criteria were adopted: Global Horizontal Irradiation (GHI), slope, aspect, land-cover suitability, distance to motorways, distance to electric transmission lines, distance to urban areas, distance to waterways, industrial-zone proximity, and snow frequency. Their sources and preparation are summarised in Table 1.

All datasets were spatially harmonised prior to analysis: reprojected to a common coordinate reference system (WGS84 / UTM Zone 33N), clipped to the study boundary, and resampled to a common 30 m grid. Vector features were rasterised where necessary, and distance-based criteria were generated as Euclidean distance rasters (Malczewski, 2006). A master restriction mask uniformly excluded non-developable areas (protected areas, water bodies, transportation corridors, and built-up zones), producing a co-registered set of criteria layers for the standardisation procedure described next.

3. Methodology

3.1 Criteria Standardisation and Reclassification

The ten criteria were originally expressed in heterogeneous units and scales: irradiation (kWh/m^2/year), terrain angles and orientation classes, land-cover categories, Euclidean distances in metres, and snow frequency. Criteria on incommensurable scales and with differing suitability directions cannot be aggregated directly, so each was transformed onto a common suitability scale and direction before weighting. All criteria were reclassified into an ordinal scale from 0 to 5, where 0 marks restricted or unsuitable cells excluded from the analysis and 1–5 represent increasing suitability, so that every valid criterion follows the same benefit direction in which a higher value indicates higher suitability.

This conversion harmonises the differing native directions of the criteria. GHI was treated as a benefit criterion (higher irradiation $\rightarrow$ higher suitability), slope so that gentle gradients scored high and steep terrain scored low or was excluded, and aspect by exposure, favouring solar-favourable orientations. Land-cover suitability followed class compatibility, with developable classes favoured and incompatible or protected classes excluded. Among infrastructure criteria, electric-line and motorway distance rewarded better grid connection and accessibility, whereas urban distance penalised immediate adjacency to built-up land while favouring moderate separation; waterway distance excluded environmental buffers and rewarded safer distances, and industrial-zone proximity rewarded nearness to productive land use. Snow frequency was a cost criterion, with lower persistence scoring higher. Thresholds followed literature guidance, planning constraints, and the empirical distribution of each layer.

In parallel, restricted cells corresponding to protected areas, water bodies, transportation corridors, and built-up zones were excluded using the master restriction mask and assigned a value of 0 or NoData prior to subsequent modelling. This procedure produced ten co-registered standardised criteria rasters on the same 30 m grid, sharing a common spatial extent and suitability direction, and ready for hybrid weighting and MCDM aggregation.

3.2 Hybrid AHP–Machine Learning Weighting Framework

To reduce reliance on purely subjective expert judgment while preserving interpretability, a hybrid weighting strategy was adopted that integrates expert-derived weights from the Analytic Hierarchy Process (AHP) with data-driven feature importance from a machine-learning analysis of existing PV installations.

The expert component was derived using AHP (Saaty, 1990). Pairwise comparisons among the ten criteria were specified on Saaty's fundamental scale, and the expert weight vector was

https://doi.org/10.5194/isprs-archives-L-4-W3-2026-1-2026

Criterion	Source	Type / Resolution	Processing / Role
GHI	SARAH-2 (CM SAF, EUMETSAT)	Raster, ≈5 km	Resampled; solar resource
Slope	SRTM DEM	DEM, 30 m	DEM-derived; terrain constraint
Aspect	SRTM DEM	DEM, 30 m	DEM-derived; solar exposure
Land-cover suitability	ESA WorldCover	Raster, 10 m	Reclassified; land-use compatibility
Motorway distance	Abruzzo Region Open Data	Vector	Euclidean distance raster; accessibility
Electric-line distance	Abruzzo Region Open Data	Vector	Euclidean distance raster; grid connection
Urban distance	ESA WorldCover (built-up)	Raster	Built-up extraction; distance raster
Waterway distance	Abruzzo Region Open Data	Vector	Euclidean distance raster; environmental buffer
Industrial-zone proximity	Abruzzo Region Open Data	Vector	Distance raster; productive land use
Snow frequency	Sentinel-2 SR (Google Earth Engine)	Raster, 20 m	NDSI snow detection, 2017–2024

Table 1. Spatial datasets and criteria used for PV suitability analysis.

obtained as the principal eigenvector of the normalised comparison matrix. Judgment consistency was confirmed by a consistency ratio of 0.0142, well below the 0.10 threshold.

To incorporate empirical deployment patterns, the machine-learning component used the locations of existing PV installations within the study area. A total of 72 existing PV plants were digitised from high-resolution satellite imagery as presence samples, and 720 background (pseudo-absence) samples were randomly generated within the developable area (1:10 ratio; 792 samples total). The ten standardised criteria values were extracted at each sample point to link observed PV occurrence with local environmental, topographic, and infrastructural conditions. An XGBoost classifier (Chen and Guestrin, 2016) was trained to separate PV presence from background and evaluated using ROC–AUC under spatial blocked cross-validation (5 outer folds over 10 coordinate-based spatial blocks, 3-fold inner tuning, fold-wise SHAP), which reduces optimistic bias from spatial autocorrelation and prevents importance leakage. The model achieved a mean ROC–AUC of 0.9391 ± 0.0312, indicating strong discrimination. SHAP (SHapley Additive exPlanations) values (Lundberg and Lee, 2017) estimated each criterion's contribution to the model output, and mean absolute SHAP values were normalised to sum to one. Urban distance and slope received the highest SHAP-derived weights, indicating the strongest data-driven influence. The model was used only to derive feature-importance weights, not to generate the suitability map directly.

The expert and empirical weights were combined through a convex linear combination. For each criterion i, the hybrid weight is defined as

$$w_i^{Hybrid} = \alpha\, w_i^{AHP} + (1-\alpha)\, w_i^{ML} \tag{1}$$

where w_i^{AHP} is the AHP expert weight, w_i^{ML} is the machine-learning feature-importance weight, and α is the mixing coefficient balancing the two. The AHP and ML weights were each normalised to sum to one before integration, and the hybrid weights were likewise normalised so that $\sum_i w_i = 1$.

The mixing coefficient α was evaluated across $\alpha \in 0.1, 0.2, \ldots, 0.9$; $\alpha = 0.7$ was selected as a compromise that retained AHP dominance while incorporating the ML-derived deployment signal (70% AHP, 30% machine learning). The resulting AHP, ML, and hybrid weights for all ten criteria are reported in Table 2 and were then applied to the standardised layers through SAW, TOPSIS, and VIKOR to generate the suitability maps described next.

Criterion	AHP weight	ML weight	Hybrid weight
GHI	0.2879	0.0820	0.2261
Slope	0.1589	0.3367	0.2122
Aspect	0.0411	0.0309	0.0380
Land-cover suitability	0.1655	0.0254	0.1234
Motorway distance	0.0847	0.0120	0.0628
Electric-line distance	0.1017	0.0172	0.0763
Urban distance	0.0254	0.4030	0.1386
Waterway distance	0.0159	0.0129	0.0150
Industrial-zone proximity	0.0673	0.0562	0.0639
Snow frequency	0.0515	0.0236	0.0431

Table 2. AHP, ML, and hybrid weights for the PV criteria.

3.3 MCDM Suitability Mapping using SAW, TOPSIS, and VIKOR

The hybrid weights were applied to the ten standardised layers to generate continuous PV suitability surfaces. Three aggregation methods were used: Simple Additive Weighting (SAW), Technique for Order Preference by Similarity to Ideal Solution (TOPSIS), and VIKOR. These methods were used to examine whether the spatial pattern changes under different aggregation logics while the weighting scheme is held fixed.

SAW, implemented as a weighted overlay, computes a weighted linear combination of the standardised layers and is directly interpretable, since the suitability score increases with the weighted contribution of favourable criteria (Malczewski, 2006). For each pixel i, the suitability score is

$$S_i = \sum_{j=1}^{n} w_j\, r_{ij} \tag{2}$$

where S_i is the suitability score of pixel i, w_j is the hybrid weight of criterion j, and r_{ij} is its standardised suitability value. TOPSIS ranks each pixel by its relative closeness to an ideal suitable condition and its distance from an undesirable one, evaluating suitability against the best and worst criterion combinations (Hwang and Yoon, 1981). VIKOR is a compromise-ranking method balancing group utility and individual regret with the standard compromise parameter v = 0.5, suited to conflicting criteria (Opricovic and Tzeng, 2004). Because lower raw VIKOR (Q) values indicate better alternatives, the VIKOR output was inverted during normalisation where required, so that all final surfaces followed the same benefit direction.

All three methods were applied at raster-cell level using the same standardised layers, hybrid weights, and analysis mask, with restricted and NoData cells excluded consistently, producing three continuous surfaces: the SAW suitability score, the TOPSIS closeness coefficient, and the inverted VIKOR suitability score, which were normalised to a common direction and classified for map visualisation and robustness assessment.

Because the three methods use different scales, comparison relied on spatial patterns and robustness measures rather than raw score magnitudes; these baseline surfaces fed the Monte Carlo and Tornado analyses.

3.4 Uncertainty and Sensitivity Analysis

Robustness was evaluated with two complementary procedures: a Monte Carlo analysis propagating weight uncertainty, and a Tornado-style one-at-a-time sensitivity analysis ranking individual criteria.

3.4.1 Monte Carlo Weight Uncertainty Propagation The baseline hybrid weights were perturbed using Dirichlet sampling centred on the original weight vector with a concentration parameter $\kappa = 100$. This generated non-negative stochastic weight sets that preserved unit summation while allowing moderate deviations around the baseline weights. For each of 1,000 realisations, SAW, TOPSIS, and VIKOR were recomputed using the same standardised layers and analysis mask, with restricted and NoData cells excluded consistently. From the ensemble, the mean, standard deviation, and coefficient of variation (CV) maps were derived for each method, with CV defined as

$$CV = \frac{\sigma}{\mu} \tag{3}$$

where σ is the standard deviation and μ is the mean suitability score across all simulations. Lower CV values indicate greater spatial stability, while higher CV values indicate greater sensitivity to weight perturbation.

In each simulation the top-suitability zone was identified using a fixed top-20% threshold of the developable area, and the frequency with which each pixel fell within this zone was recorded as a top-20% suitability probability map; pixels with high selection probability represent robust candidate areas. The broader top-20% threshold delineates a planning-scale priority zone, whereas the Tornado analysis uses a tighter top-10% to test sensitivity within the highest-priority core.

3.4.2 Tornado-Style One-at-a-Time Sensitivity Analysis To identify the criteria that most strongly control the spatial stability of the high-suitability zones, each criterion weight was perturbed individually by $\pm 10\%$, all weights were renormalised to sum to one, and SAW, TOPSIS, and VIKOR were recalculated. The induced change was quantified over the top-10% suitability zone, with the impact of each perturbation defined as

$$\text{Impact} = 1 - J \tag{4}$$

where J is the Jaccard overlap between the baseline top-10% zone and the perturbed top-10% zone. Higher impact values denote larger Jaccard overlap loss and therefore a greater spatial change caused by perturbing that criterion, providing a criterion-influence ranking for each aggregation method.

Together, these outputs quantify the robustness of the hybrid-weighted surfaces under criterion-weight uncertainty, as presented next.

4. Results and Discussion

4.1 Hybrid Weighting Outcomes and Baseline Suitability Patterns

The hybrid weights (Table 2) concentrate on four criteria: GHI (0.226), slope (0.212), urban distance (0.138), and land-cover suitability (0.123), together about 70% of the total. PV suitability across the province is therefore governed mainly by solar resource, terrain, settlement proximity, and land use. The two source components disagree sharply. AHP ranks GHI highest (0.287), reflecting the expert view that irradiation is the leading physical control, whereas the XGBoost–SHAP component favours urban distance (0.403) and slope (0.336) and down-weights GHI to 0.082. This shows that the 72 existing plants sit on gentle terrain at moderate distance from built-up land rather than where irradiation peaks, which varies little across the developable area. The hybrid scheme ($\alpha = 0.7$) keeps GHI physically important while raising slope and urban distance toward the observed deployment pattern.

Applying these weights through SAW, TOPSIS, and VIKOR produces the suitability maps in Fig. 3. The three surfaces agree on the broad pattern: the highest-suitability classes cluster on flat, accessible valley floors and intermontane basins, while steep terrain and restricted land are excluded. These cores lie close to settlements; because the master mask already removes built-up land, they represent developable peri-urban ground, not the urban fabric itself, although they carry a higher risk of land-use competition that local planning must weigh. Differences between the methods are local and follow each aggregation logic.

4.2 Spatial Robustness under Criterion-Weight Uncertainty

Because the same Dirichlet perturbation scheme was applied to all three methods across the 1,000 simulations, differences in output stability mainly reflect how each aggregation method responds to the same weight uncertainty. The Monte Carlo summary (Table 3) shows a clear stability gradient: the mean coefficient of variation (CV) is lowest for SAW (0.046), intermediate for TOPSIS (0.121), and highest for VIKOR (0.193), so SAW scores are least affected by weight perturbation and

Method	Mean	Mean SD	Mean CV
SAW	2.889	0.131	0.046
TOPSIS	0.393	0.047	0.121
VIKOR	0.517	0.091	0.193

Table 3. Monte Carlo summary statistics over 1,000 weight-perturbation simulations.

VIKOR most. Raw means are not compared directly because the methods use different scales; the dimensionless CV is more appropriate for comparing relative stability. The CV maps (Fig. 4) show where this uncertainty is spatially concentrated. SAW gives low, fairly uniform CV across the developable area; TOPSIS shows moderate variability, more stable in the main high-suitability basins and higher toward marginal areas; and VIKOR shows the highest, most clustered CV values, indicating that its compromise-ranking structure is most sensitive to weight perturbation. This is consistent with the aggregation logic: SAW combines criteria linearly, so weight changes produce roughly proportional score changes, whereas the ideal-solution and compromise-ranking mechanisms in TOPSIS and VIKOR can amplify changes near ranking thresholds.

4.3 Stability of High-Suitability Zones across Simulations

The top-20% probability maps (Fig. 5) record how often each pixel fell within the top-suitability zone across the 1,000 simulations. Pixels near 1 form robust high-suitability cores, those near 0 stay outside, and intermediate values mark transitional areas that move in and out of the top zone as weights change. The robust cores are spatially concentrated rather than scattered, occurring mainly in the gentle, accessible intermontane basins and valley floors identified in Section 4.1.

Across the three methods the cores occupy largely similar locations, indicating that priority PV zones remain stable under both weight perturbation and aggregation method. The VIKOR pattern is slightly more fragmented along the margins, consistent with its higher CV (Section 4.2), though the same basins remain most suitable. These persistent cores are the most defensible candidate zones, while the transitional band marks sensitivity-prone sites needing closer review. As a consistency check, the 72 existing plants were overlaid on the probability maps; because the mask removes built-up land (including plant footprints), suitability was read from the nearest developable pixel within 1 km (62 plants matched). Of these, 65% (SAW) and 60% (TOPSIS) lay within the robust zone (probability ≥ 0.5) versus 45% (VIKOR), agreeing with observed siting for SAW and TOPSIS. This is a consistency check, not independent validation, as the ML weights derive from the same plants.

4.4 Criterion Influence on Suitability Stability: Tornado Sensitivity Analysis

The Tornado analysis (Fig. 6) measures how much the top-10% suitability zone shifts when each criterion weight is perturbed by $\pm 10\%$ one at a time, expressed as Jaccard overlap loss. A few criteria dominate, and which one leads depends on the aggregation logic: slope (0.059) and GHI (0.058) in SAW, urban distance (0.166) well ahead of GHI (0.110) in TOPSIS, and GHI (0.102) about twice urban distance (0.051) in VIKOR. GHI and urban distance stay influential across all three methods, whereas snow frequency, aspect, and waterway distance barely move the high-priority zone. Critically, the most influential criteria (GHI, urban distance, and slope) are the same ones for which AHP and machine-learning weights diverge most (Section 4.1), so hybrid weighting is most consequential exactly where it changes the spatial outcome. Weight refinement and uncertainty assessment should therefore focus on these criteria, while lower-sensitivity criteria are retained for environmental, physical, and regulatory completeness.

5. Conclusion

This study developed a hybrid AHP–machine-learning weighting framework for GIS-based PV suitability mapping in the Province of L'Aquila and extended it with an explicit assessment of spatial robustness under criterion-weight uncertainty. The hybrid scheme ($\alpha = 0.7$) combined internally consistent expert weights (AHP consistency ratio = 0.0142) with data-driven feature importance from an XGBoost model trained on 72 existing PV plants (ROC–AUC = 0.9391). The two components differed most for GHI, urban distance, and slope, which the hybrid weighting reconciled while preserving interpretability.

The robustness analysis produced three consistent findings. First, Monte Carlo simulation revealed a clear, aggregation-driven stability gradient (mean CV = 0.046, 0.121, 0.193 for

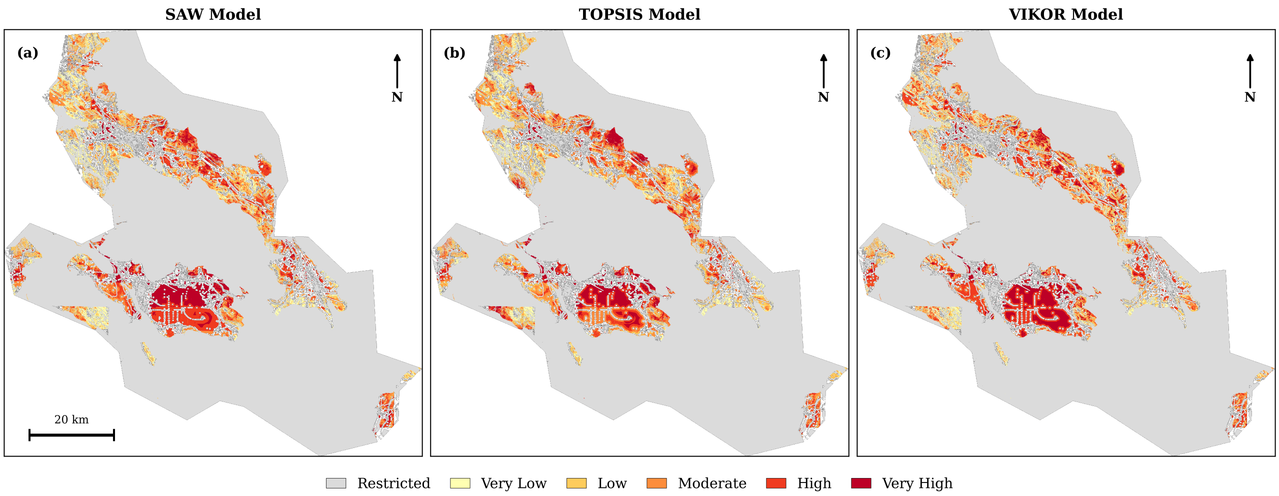

Figure 3. Baseline hybrid-weighted PV suitability maps: (a) SAW, (b) TOPSIS, and (c) VIKOR. Suitability classes range from Very Low to Very High; restricted (non-developable) land is masked in grey.

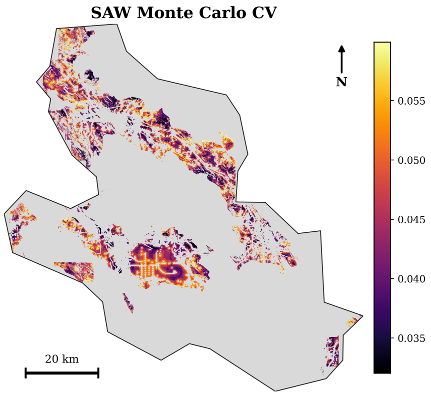

Figure 4. Spatial coefficient of variation (CV $= \sigma/\mu$) maps from 1,000 Monte Carlo simulations for SAW, TOPSIS, and VIKOR; lower values indicate stable suitability, higher values indicate sensitivity to criterion-weight uncertainty.

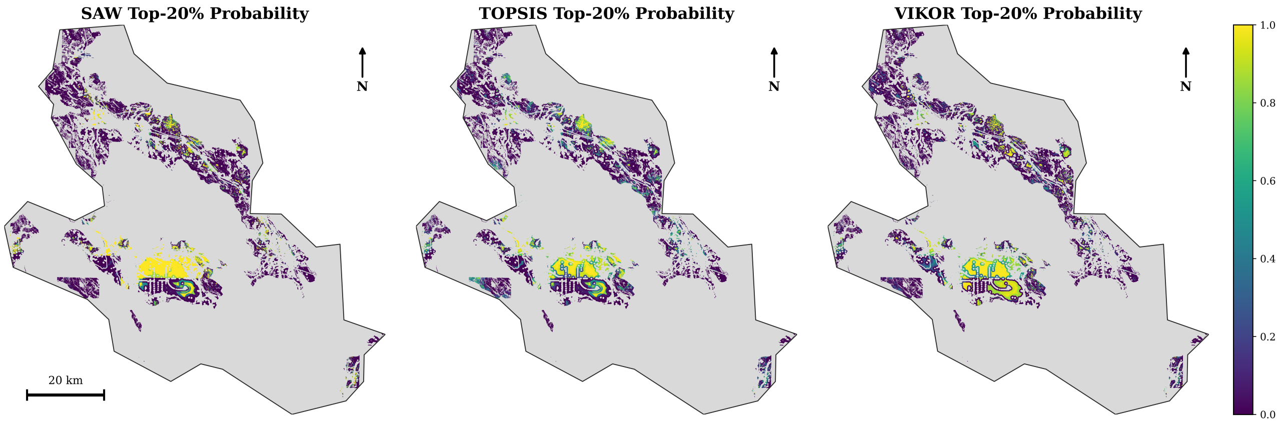

Figure 5. Top-20% suitability probability maps from 1,000 Monte Carlo simulations for SAW, TOPSIS, and VIKOR; higher pixel values indicate spatially robust candidate sites.

SAW, TOPSIS, VIKOR). Second, the top-suitability probability maps identified concentrated high-suitability cores in accessible valley areas. These cores persisted across all weight perturbations and all three methods. Third, the Tornado analysis identified GHI, urban distance, and slope as the dominant controls on this stability, the same criteria where expert and data-driven weights diverged most, confirming that hybrid weighting matters most for the variables that govern the spatial outcome. A check against the 72 existing plants confirmed that the SAW and TOPSIS robust zones broadly coincide with observed siting.

Taken together, the framework moves beyond a single deterministic map by distinguishing robust priority zones from sensitivity-prone transitional areas and ranking the criteria that most affect spatial stability, giving a more defensible, uncertainty-aware basis for PV siting. The workflow is transferable to regions with comparable geospatial data, provided the training samples, criterion thresholds, and derived weights are recalibrated to local deployment patterns and planning conditions.

References

Al Garni, H. Z., Awasthi, A., 2020. A monte carlo approach applied to sensitivity analysis of criteria impacts on solar PV site selection. *Handbook of Probabilistic Models*, Butterworth-Heinemann, 489–504.

Ali, K., Clementini, E., Patrizi, R., Santic, M., Villante, C., 2025a. Multi-Sensor Deep Learning Framework for LST Downscaling and Scaling Effect Assessment in Heterogeneous Urban Landscapes. *The International Archives of the Photogrammetry, Remote Sensing and Spatial Information Sciences*, 48, 1–8.

Ali, K., Clementini, E., Patrizi, R., Santic, M., Villante, C., 2026. CNN-Based Downscaling of Land Surface Temperature and Scaling Effect Analysis Using Multi-Sensor Satellite Data: A Case Study in L'Aquila, Italy. *The International Archives of the Photogrammetry, Remote Sensing and Spatial Information Sciences*, 48, 35–42.

Ali, K., Ullah, S., Clementini, E., 2025b. Robust Backstepping Super-Twisting MPPT Controller for Photovoltaic Systems Under Dynamic Shading Conditions. *Energies*, 18(19), 5134.

Aydin, N. Y., Kentel, E., Duzgun, H. S., 2013. GIS-Based Site Selection Methodology for Hybrid Renewable Energy Systems: A Case Study from Western Turkey. *Energy Conversion and Management*, 70, 90–106.

Chen, T., Guestrin, C., 2016. XGBoost: A scalable tree boosting system. *Proceedings of the 22nd ACM SIGKDD International Conference on Knowledge Discovery and Data Mining (KDD '16)*, ACM, San Francisco, CA, USA, 785–794.

Clementini, E., Patrizi, R., Santic, M., Villante, C., 2024. A Geo-Spatial Information System for Photovoltaic Plants Development and Monitoring. *The International Archives of the Photogrammetry, Remote Sensing and Spatial Information Sciences*, 48, 45–50.

Feizizadeh, B., Blaschke, T., 2014. An Uncertainty and Sensit-

https://doi.org/10.5194/isprs-archives-L-4-W3-2026-1-2026

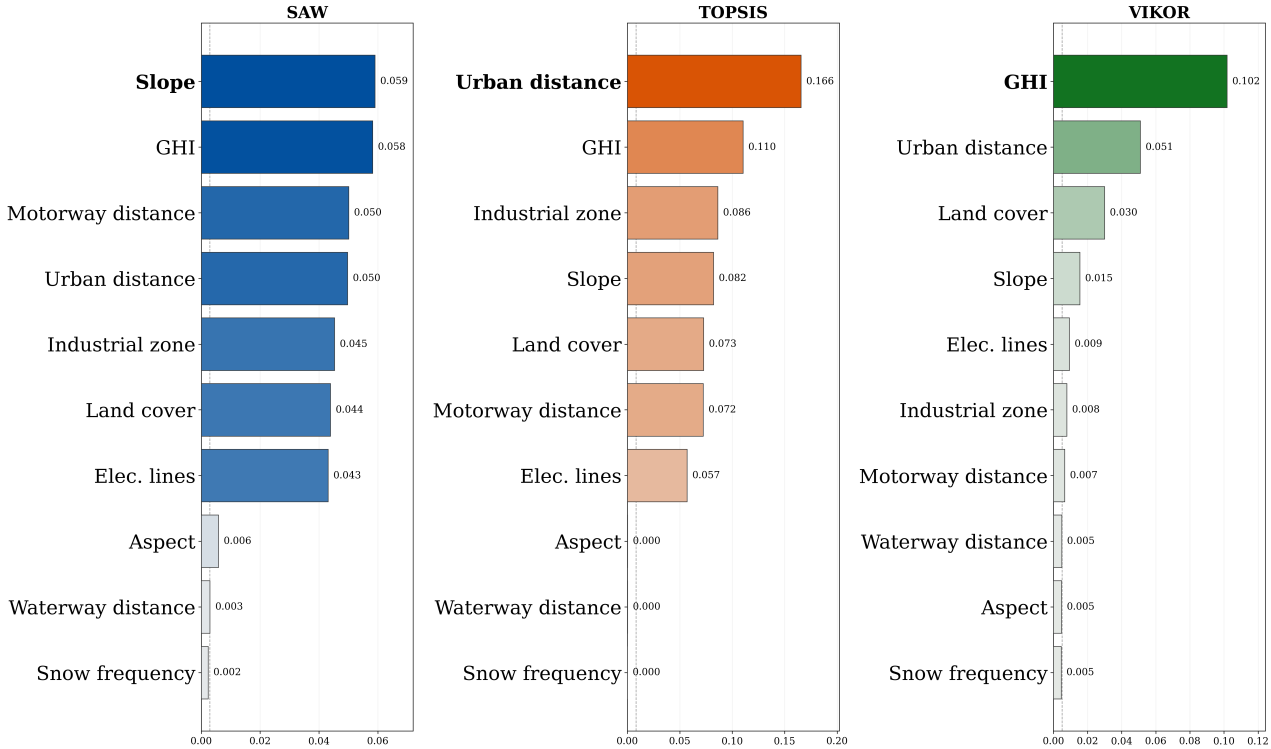

Figure 6. Tornado sensitivity results for SAW, TOPSIS, and VIKOR; bars show Jaccard overlap loss $(1 - J)$ in the top-10% suitability zone under $\pm 10\%$ weight perturbation per criterion.

ivity Analysis Approach for GIS-Based Multicriteria Landslide Susceptibility Mapping. *International Journal of Geographical Information Science*, 28(3), 610–638.

Hanna, R., Heptonstall, P., Gross, R., 2024. Job Creation in a Low Carbon Transition to Renewables and Energy Efficiency: A Review of International Evidence. *Sustainability Science*, 19(1), 125–150.

Hastie, T., Tibshirani, R., Friedman, J., 2009. *The Elements of Statistical Learning: Data Mining, Inference, and Prediction*. 2nd edn, Springer, New York.

Heo, J., Moon, H., Chang, S., Han, S., Lee, D.-E., 2021. Case Study of Solar Photovoltaic Power-Plant Site Selection for Infrastructure Planning Using a BIM-GIS-Based Approach. *Applied Sciences*, 11(18), 8785.

Hosouli, S., Hassani, R. A., 2024. Application of Multi-Criteria Decision Making (MCDM) Model for Solar Plant Location Selection. *Results in Engineering*, 24, 103162.

Hwang, C.-L., Yoon, K., 1981. *Multiple Attribute Decision Making: Methods and Applications*. Springer-Verlag, Berlin.

IRENA, 2024. Renewable power generation costs in 2023. Technical report, International Renewable Energy Agency, Abu Dhabi.

Ligmann-Zielinska, A., Jankowski, P., 2014. Spatially-Explicit Integrated Uncertainty and Sensitivity Analysis of Criteria Weights in Multicriteria Land Suitability Evaluation. *Environmental Modelling & Software*, 57, 235–247.

Lundberg, S. M., Lee, S.-I., 2017. A unified approach to interpreting model predictions. *Advances in Neural Information Processing Systems (NIPS)*, 30, 4765–4774.

Malczewski, J., 2006. GIS-Based Multicriteria Decision Analysis: A Survey of the Literature. *International Journal of Geographical Information Science*, 20(7), 703–726.

Merrouni, A. A., Elwali Elalaoui, F., Ghennioui, A., Mezrhab, A., Mezrhab, A., 2018. A GIS-AHP Combination for the Sites Assessment of Large-Scale CSP Plants with Dry and Wet Cooling Systems. Case Study: Eastern Morocco. *Solar Energy*, 166, 2–12.

Opricovic, S., Tzeng, G.-H., 2004. Compromise Solution by MCDM Methods: A Comparative Analysis of VIKOR and TOPSIS. *European Journal of Operational Research*, 156(2), 445–455.

Rudin, C., 2019. Stop Explaining Black Box Machine Learning Models for High Stakes Decisions and Use Interpretable Models Instead. *Nature Machine Intelligence*, 1(5), 206–215.

Saaty, T. L., 1990. How to Make a Decision: The Analytic Hierarchy Process. *European Journal of Operational Research*, 48(1), 9–26.

Sahoo, S. K., Choudhury, B. B., Dhal, P. R., Hanspal, M. S., 2025. A Comprehensive Review of Multi-Criteria Decision-Making (MCDM) Toward Sustainable Renewable Energy Development. *Spectrum of Operational Research*, 2(1), 309–325.

Sari, F., Yalcin, M., 2024. Investigation of the Importance of Criteria in Potential Wind Farm Sites via Machine Learning Algorithms. *Journal of Cleaner Production*, 435, 140575.

Sun, Y., Zhu, D., Li, Y., Wang, R., Ma, R., 2023. Spatial Modelling the Location Choice of Large-Scale Solar Photovoltaic Power Plants: Application of Interpretable Machine Learning Techniques and the National Inventory. *Energy Conversion and Management*, 289, 117198.

UNFCCC, 2023. Report of the conference of the parties on its twenty-eighth session (cop28). Dubai, 30 November–13 December 2023. `https://unfccc.int/documents/637067`.

Villacreses, G., Martínez-Gómez, J., Jijón, D., Cordovez, M., 2022. Geolocation of Photovoltaic Farms Using GIS with Multiple-Criteria Decision-Making (MCDM) Methods: Case of the Ecuadorian Energy Regulation. *Energy Reports*, 8, 3526–3548.